Vol. 26 • No. 28 • July 23 • 2014

D10488

www.advmat.de

ADVANCED MATERIALS

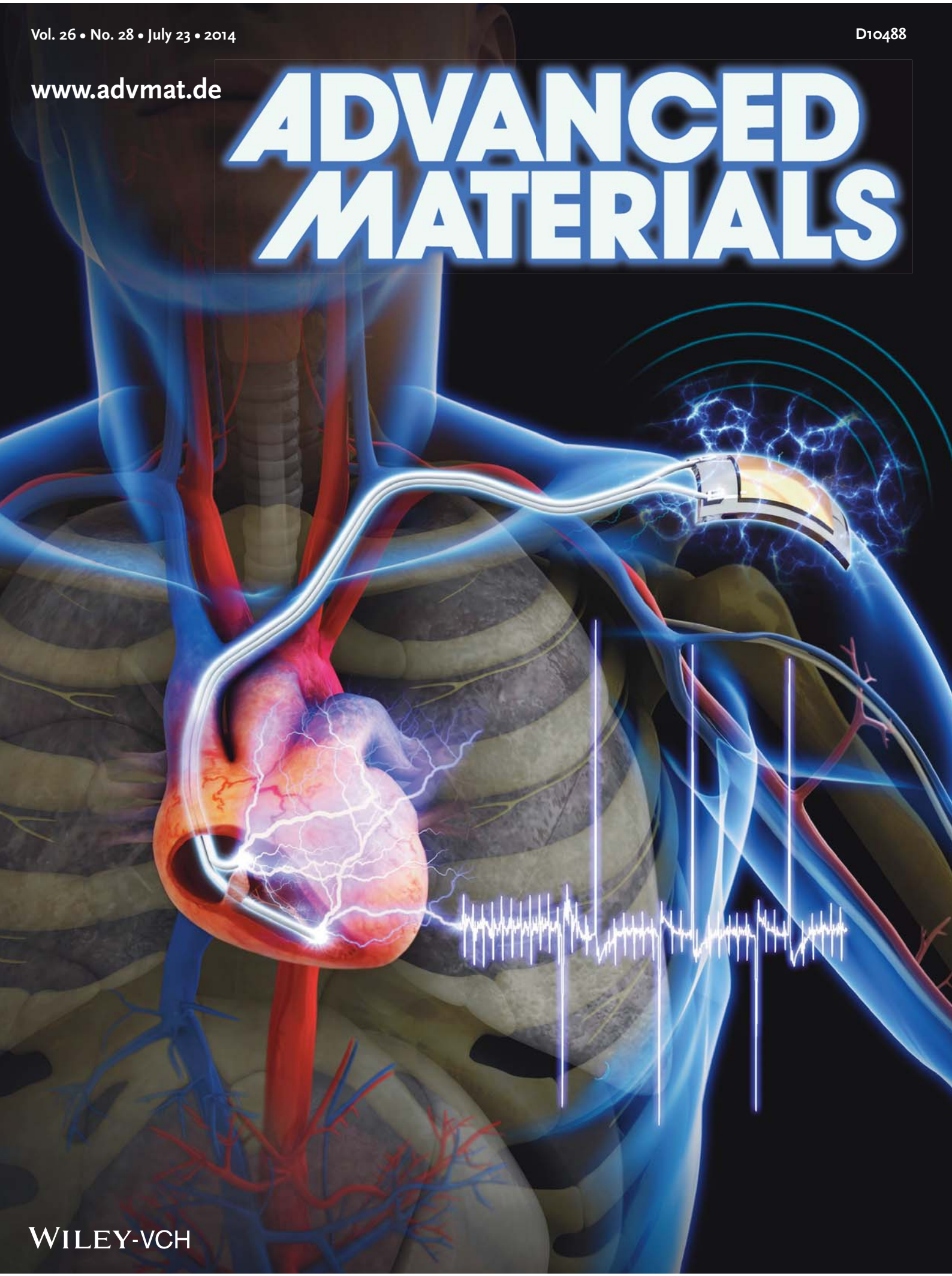

WILEY-VCH

ADVANCED MATERIALS
www.advmat.de

www.MaterialsViews.com

Self-Powered Cardiac Pacemaker Enabled by Flexible Single Crystalline PMN-PT Piezoelectric Energy Harvester

*Geon-Tae Hwang, Hyewon Park, Jeong-Ho Lee, SeKwon Oh, Kwi-Il Park, Myunghwan Byun, Hyelim Park, Gun Ahn, Chang Kyu Jeong, Kwangsoo No, HyukSang Kwon, Sang-Goo Lee, Boyoung Joung, and Keon Jae Lee**

Artificial cardiac pacemakers have made a significant contribution to regulate heartbeat using electrical impulses for contracting the heart muscles of people who suffer from sick sinus syndrome or heart block which causes abnormal heart rate, and may result in symptoms including syncope, angina, dizziness, and even heart failure or heart attack.[1,2] However, due to the limited lifespan of the battery, replacement surgery for the artificial pacemaker implanted beneath chest skin should be made every 7 to 10 years [or even every 3 to 6 years for an implantable cardioverter defibrillator (ICD)].[3,4] This poses a risk to elderly persons, particularly with regard to infection or bleeding during the surgical procedure.[5] Enhancing the battery lifetime is thus a critical issue to assure longer working time of the implanted pacemakers, and increase the replacement cycle. An attractive approach to address this challenge is to adopt self-powered systems, which potentially can provide low maintenance, independent operation, and sustainability for implantable biomedical devices.[6,7]

Energy harvesting systems based on irregular vibrational motion and mechanical deformation are promising candidates for self-powered biomedical electronics.[8–12] Manipulating flexible piezoelectric energy harvesters [called nanogenerators (NGs)] inside the human body is of particularly medical interest, because they can scavenge inexhaustible biomechanical energy such as cardiac motion, muscle contraction/relaxation, and blood circulation and convert it to electrical energy.[13] This could feasibly contribute to not only the operation of implantable heart rate monitoring and transmitting system, but also the development of a self-powered artificial pacemaker by directly recharging the battery or stimulating the heart.[14,15] Many research teams including our group have explored various types of flexible piezoelectric materials on thin plastic substrates including ZnO nanowires,[16,17] $BaTiO_3$ thin film,[18] and lead zirconatate titanate (PZT) thin films.[19,20] Although the aforementioned flexible energy harvesters can provide power for operating small electronic devices, their relatively low output current of a few μA has severely restricted the range of applications in consumer electronics as well as biomedical devices: for example, a cardiac pacemaker operates at an input of 100 μA and 3 V.[17,21]

Therefore, it is highly desirable to utilize materials with a high piezoelectric charge coefficient, which represents the piezoelectric capability of converting mechanical deformation into electric charges, to increase the output current efficiency for flexible energy harvesters. One such piezoelectric material is a new generation of single crystalline (1-x) $Pb(Mg_{1/3}Nb_{2/3})O_3$ – $xPbTiO_3$ (PMN-PT). It has exceptional piezoelectric charge constant of d_{33} up to 2500 pC/N, which is almost 4 times higher than that of PZT, 20 times higher than that of $BaTiO_3$, and 90 times higher than that of ZnO.[22,23]

Herein, we report a flexible and highly-efficient energy harvester enabled by single crystalline piezoelectric PMN-PT thin film on a plastic substrate to achieve a self-powered artificial pacemaker with significantly increased electric output current. The stress-controlled exfoliating process was optimized for transferring the PMN-PT thin film from a bulk substrate onto a flexible substrate without mechanical damage by utilizing the inherent residual stress of Ni film.[24] The maximum output current and voltage of the flexible PMN-PT thin film harvester reached 145 μA and 8.2 V, respectively, through the periodic mechanical motions of bending and unbending. Furthermore, current signal of 223 μA, corresponding to the highest output current among piezoelectric-based flexible NGs reported to date, was obtained by finger tapping. The converted electricity was used to directly turn on 50 commercial green light emitting diodes (LEDs) and charge coin batteries for driving portable electronic devices. Finally, real-time functional electrical stimulation was performed to provide the artificial heart beating for a live rat using the high-performance flexible PMN-PT energy harvester.

Figure 1a schematically illustrates the device fabrication process and stimulation test on a living heart. The following is a detailed explanation: (i) Single crystalline rhombohedral 0.72 PMN - 0.28 PT ingot was grown directly from the melt by a modified Bridgman method near the morphotropic

G.-T. Hwang, S. Oh, K.-I. Park, Dr. M. Byun, G. Ahn, C. K. Jeong, Prof. K. No, Prof. H. Kwon, Prof. K. J. Lee
Department of Materials Science and Engineering
Korea Advanced Institute of Science and Technology (KAIST)
291 Daehak-ro, Yuseong-gu, Daejeon 305-701, Republic of Korea
E-mail: keonlee@kaist.ac.kr

H. Park, H. Park, Prof. B. Joung
Division of Cardiology
Brain Korea 21 PLUS Project for Medical Science
Yonsei University College of Medicine
50 Yonsei-ro, Seodaemun-gu, Seoul 120-752, Republic of Korea

J.-H. Lee, Dr. S.-G. Lee
iBULe Photonics Co., Ltd.
145 Gaetbeol-ro, Yeonsu-gu, Incheon 406-840, Republic of Korea

DOI: 10.1002/adma.201400562

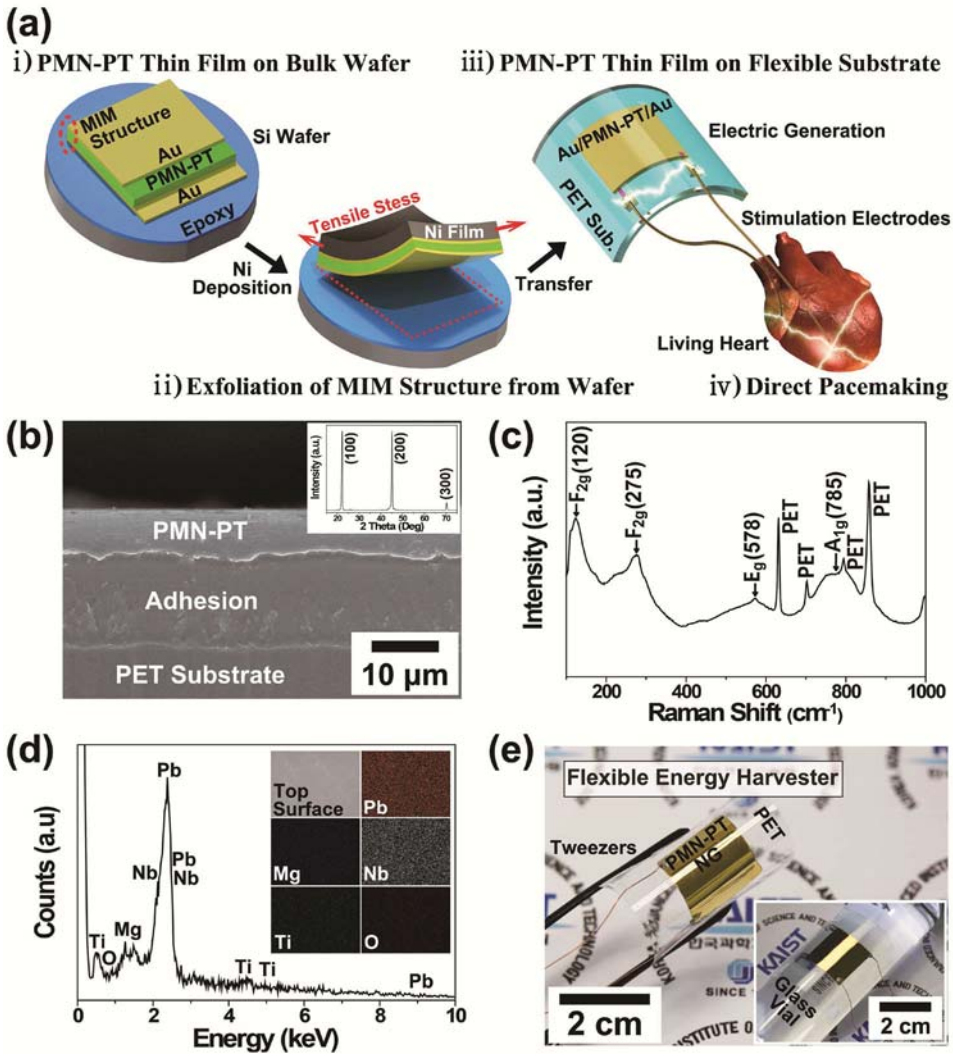

Figure 1. (a) Schematic illustration of the fabrication process and biomedical application of flexible PMN-PT piezoelectric energy harvester. (b) Cross-sectional SEM image of the PMN-PT thin film on a PET substrate. The inset shows an XRD pattern of PMN-PT thin film. (c) Raman spectrum obtained from PMN-PT thin film. The indexed sharp spectra agrees well with the typical feature of perovskite PMN-PT. (d) EDS curve analyzed from the top surface of PMN-PT thin film. The insets show the EDS elemental mapping result. (e) Photograph of flexible PMN-PT thin film energy harvester on a PET substrate. The inset presents that the NG device provides conformal contact on curvilinear surface of glass vial.

phase boundary (MPB).[25,26] Exceptionally high piezoelectric and electromechanical coupling coefficients were achieved at a composition around MPB with a single crystal structure.[27] The (001)-oriented PMN-PT crystal was cut into a square block and polished to have a mirror surface using a diamond suspension. An Au bottom electrode deposited PMN-PT plate was completely bonded on (100) silicon wafer by adhesive epoxy and then thinned to a film thickness of 8.4 μm using grinding and subsequent chemical mechanical polishing (CMP). The PMN-PT was poled along the [100] direction by applying an electric field of 1.8 kV/mm at room temperature for 1 hour followed by deposition of the top electrode layer. (ii) A mechanical exfoliating process was carried out to peel off the top piezoelectric portion of the PMN-PT metal-insulator-metal (MIM) layer (8.6 μm in thickness) from the silicon substrate using an electroplated tensile Ni stressor. Exploiting the directional stress mismatch between the top Ni film (intrinsic tensile stress) and underlying layers (against compressive stress) of the MIM/epoxy/wafer, offered a simple and robust route to spontaneous and uniform exfoliation of the piezoelectric thin film from the mother substrate without mechanical damage such as cracking, delamination, or wrinkling.[24] Moreover, the thickness of the exfoliated PMN-PT can be readily controlled by modulating the residual stress of the Ni film,[28] and a 20 μm thick Ni layer was an optimized condition for safe and precise detachment of the piezoelectric MIM structure.[24] (iii) The large-area PMN-PT thin film (1.7 cm × 1.7 cm) was transferred onto ultraviolet (UV) light cured polyurethane (PU)-coated polyethylene terephthalate (PET) substrate. The freestanding thin PMN-PT film on the thin plastic substrate provided enough flexibility to achieve conformal contact on a curved subcutaneous layer and corrugated organs in the human body, thus making it possible to serve as a self-energy generator by slight mechanical movements.[29] (iv) To stimulate a live rat's heart by the flexible

PMN-PT energy harvester, Cu wires were attached to the metal pads with a silver conductive paste and then connected to stimulation electrodes. Finally, the PMN-PT stimulator was applied as an artificial cardiac pacemaker with electrical energy generated by a periodic bending/unbending cycle of the flexible device as schematically shown in Figure 1a-iv.

Figure 1b shows a cross-sectional scanning electron microscopy (SEM) image of the single crystalline PMN-PT thin film on a flexible PET substrate after the transfer process. The PMN-PT thin film (8.4 μm in thickness) bonds on PU without the formation of cracks or blisters in the piezoelectric material. We conducted structural and compositional characterizations of the flexible PMN-PT thin film on plastics using X-ray diffraction (XRD), Raman spectroscopy, and energy dispersive spectroscopy (EDS). The inset of Figure 1b shows the results of the XRD analysis of the single crystal PMN-PT thin film with only (001)-textured peaks, confirming the formation of a pure perovskite structure.[30] Raman spectroscopy (Figure 1c) was carried out to analyze the phase of the PMN-PT thin film using a 514.5 nm Ar^+ laser as an excitation source at room temperature. The peaks of the Raman spectra at 120, 275, 578, and 785 cm^{-1} are ascribed to the F_{2g}, F_{2g}, E_g, and A_{1g} modes respectively, in good agreement with the typical features for perovskite relaxors.[27] Figure 1d and its inset show the EDS spectrum and elemental mapping results obtained from the top surface of the PMN-PT thin film. From the EDS-based compositional analysis, it is clearly proven that the single crystal PMN-PT on flexible substrate consists of all the required elements, and the Pb, Mg, Nb, Ti, and O atoms are distributed evenly across the measured area. Figure 1e shows the flexible PMN-PT energy harvester completely bent by tweezers without notable damage, and the inset presents the device on a rounded glass vial with a curvature radius of 1.4 cm. The Ni exfoliated piezoelectric thin film on a plastic substrate could provide outstanding bendability and mechanical stability for flexible NGs.[31]

PMN-PT is considered to be among the most promising piezoelectric and ferroelectric materials due to its excellent dielectric, ferroelectric, and piezoelectric characteristics.[32] To evaluate the ferroelectric properties of the flexible single crystal PMN-PT thin film, we measured its dielectric constant, dielectric loss, and polarization-electric field (P-E) hysteresis loop. **Figure 2**a shows the dielectric properties of the PMN-PT thin film on a PET substrate at room temperature as a function of frequency, ranging from 1 kHz to 1 MHz, with a direct current (DC) bias of 5 mV. The dielectric constant (blue line) and loss tangent (red line) of the PMN-PT thin film are 3500 and 0.045, respectively, at 1 kHz, and are stably preserved with increasing frequency. The inset of Figure 2a shows the dependence of the dielectric constant of MIM on the bending radius at a fixed frequency of 1 kHz. As the bending radius is varied from 60 to 10 mm (i.e., corresponding to a gradual increase of the surface strain from 0.1 to 0.62%), the dielectric constant increases up to 4280. It seems that the lattice distortion mainly governed by tensile stress possibly enhances the dielectric constant of the PMN-PT thin film with variation of the lattice polarity and lattice dynamic property.[33] The ferroelectric materials are polarized by exposing them to a strong DC electric field below the Curie point.[34] Figure 2b plots the characterized P-E hysteresis

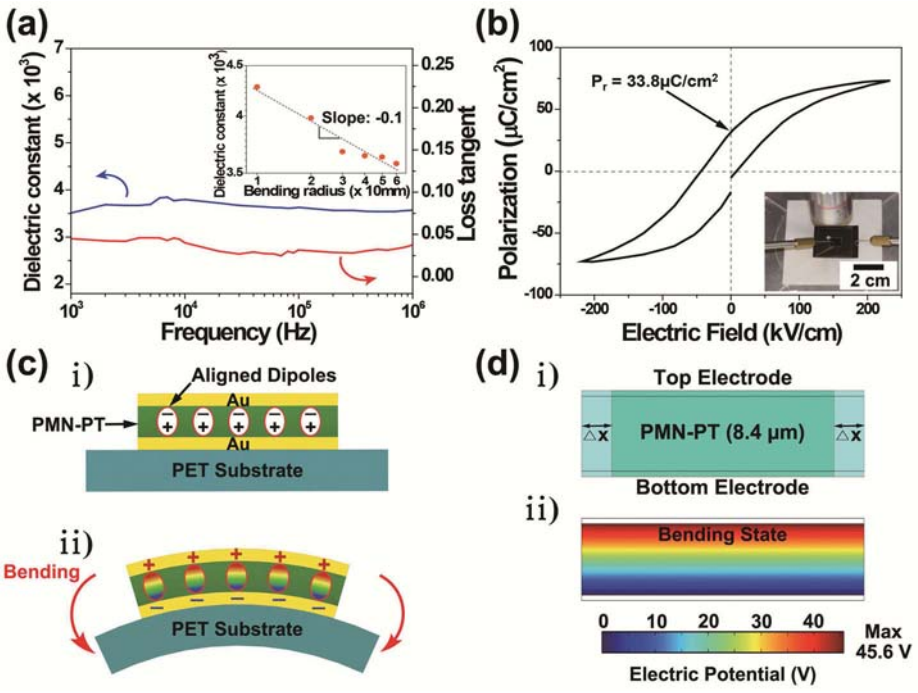

Figure 2. (a) Dielectric properties of MIM structured PMN-PT thin film as a function of frequency on a plastic substrate. The inset shows the dielectric constant changes of the flexible PMN-PT thin film at different bending radii. (b) Polarization-electric field (P-E) hysteresis loop of the ferroelectric PMN-PT thin film on a PET. The inset shows the photograph image of ferroelectric measurement on a prove station. (c) Schematics of the electricity generation of the flexible PMN-PT thin film NG before (i) and after (ii) bending. (d) The simulated model (i) and inside piezopotential distribution (ii) of the MIM-based PMN-PT energy harvester under tensile strain of 0.36%.

curve of the PMN-PT thin film on a plastic substrate at room temperature, exhibiting good ferroelectric property with a high remnant polarization (P_r) of 33.8 μC/cm^2 at a maximum applied field of 225 kV/cm.[32]

Figure 2c-i and 2c-ii schematically illustrate how electric energy is generated from the flexible energy harvester. The dipoles in the PMN-PT thin film can be aligned during the poling process under a high electric field. As depicted in the top panel of Figure 2c-i, the dipoles in the PMN-PT thin film are originally positioned perpendicular to the surface of the device. Once the flexible harvesting device is bent, as shown in Figure 2c-ii, piezopotential is generated inside the PMN-PT thin film by the tensile stress-induced deformation of the device, resulting in electrons flow in the external load to balance the electric field made by dipoles and accumulate at the top electrode. When the NG returns to the original flat state, the charges tend to move back to their original positions. Consequently, under periodic motions of bending and unbending, positive and negative electric signals are generated from the flexible device. Figure 2d shows the theoretical calculation of the piezopotential inside the PMN-PT MIM structure by a finite element analysis (FEA) using the COMSOL package to provide more information on the working principle. We simulated the piezopotential distribution for a PMN-PT thin film (8.4 μm in thickness) on a plastic substrate (120 μm in thickness) with a bending radius of 16.5 mm (i.e., corresponding to a tensile strain of 0.36%). A piezoelectric charge constant of d_{31} = −1102 pC/N, a dielectric constant of K^T = 1264, a Young's modulus of E = 133 GPa, and a mass density of ρ = 8040 kg/m^3 were used for the FEA.[35] The strain applied to the PMN-PT thin film nearly equals the strain at the top surface of the plastic film due to the thickness of plastic being sufficiently larger than the thickness of the piezoelectric film.[36] From the relationship ($S = \Delta L/L_0$) between the tensile strain (S) and the original width (L_0) on the X-axis of the flexible NG, the PMN-PT thin film is lengthened in the parallel direction for a displacement (ΔL) of 64 μm in the simulated model (Figure 2d-i). We assumed no failure modes such as cracking, slipping, or delamination of the PMN-PT thin film on plastic in the FEA.[37] As illustrated in Figure 2d-ii, the calculation predicted a piezopotential difference of 45.6 V inside the color-coded PMN-PT thin film. This FEA result strongly supports that mechanical deformation of the PMN-PT thin film can be immediately converted into electric energy.

Periodic bending/unbending motions of the flexible PMN-PT energy harvester were performed by a linear motor for a strain of 0.36% at a strain rate of 2.3%·s^{-1} (frequency of 0.3 Hz) to investigate the electric output of the harvesting device. **Figure 3**a shows three distinctively different states corresponding to the original flat state, bending state, and release state of the NG mounted on the bending stage to generate output voltage and current. As shown in Figure 3b, short-circuit current and open-circuit voltage were generated from the thin film harvester up to 145 μA and 8.2 V over a working area of 1.7 cm × 1.7 cm. Additionally, current signal of 223 μA was obtained by vertically tapping the device using human fingers (see Supporting Information, Figure S2). The exceptional output current of our device could facilitate wide application of commercial electronic devices and implantable biomedical electronics based on high current operation.[17] The experimentally measured piezopotential of the PMN-PT energy harvester (8.2 V) was lower than the simulated result of 45.6 V. This deviation is presumably due to the voltage drop resulting from internal leakage paths and charge loss in the MIM structure.[38]

It is interesting that the output current from this flexible PMN-PT NG is much greater than that generated by previously reported flexible piezoelectric NGs on plastic substrates. The maximum current of 223 μA is over 36 times larger than that (6 μA) of a ZnO nanowire NG[17] and 8500 times greater than that (26 nA) of a $BaTiO_3$ thin film NG.[18] When a piezoelectric device is deformed by mechanical stress, the generated total charge (Q) at a short-circuit system can be theoretically described by $Q = A \cdot S \cdot E \cdot d_{3j}$, where A is the surface area of the piezoelectric material, S is the strain, E is the Young's modulus, and d_{3j} is the piezoelectric charge constant induced polarization in direction 3 (Z-axis) of a three dimensional coordinate system; the subscript 'j' denotes direction 1 (X-axis) or 3 (Z-axis) of induced strain.[34] The modes of d_{31} and d_{33} are widely used for general piezoelectric applications. From the above equation, we infer that the highest d_{3j} value along with the large area of PMN-PT MIM could play critical roles in dramatically enhancing the output current of a flexible energy harvester.[22] On the other hand, there is a direct correlation between the output voltage and the piezoelectric voltage coefficient ($g_{3j} = d_{3j}/\varepsilon_0 \cdot K^T$; ε_0 is the permittivity of free space and K^T is the dielectric constant of the material). The open-circuit voltage (V) generated by the piezoelectric flexible NG is defined by $V = l \cdot S \cdot E \cdot g_{3j}$, where l is the perpendicular distance between the adjacent electrodes; the computational simulation in Figure 2d was basically derived from this equation.[22] The PMN-PT thin film energy harvester can generate higher output voltage than the similar structure of the PZT NG in theory due to the high g_{3j} value of the PMN-PT (see Supporting Information for the calculated potential distribution in a PZT-5A thin film, Figure S4).[39,40] Consequently, single crystalline PMN-PT thin film having a high piezoelectric constant is expected to provide outstanding output current and voltage to flexible thin film harvesting devices for realization of self-powered electronic systems.

The widely used switching polarity test was performed to verify that the output pulses are purely generated from the energy harvester. Once a forward connection was established between the NG and the measurement system, as depicted in the inset of Figure 3b-i, the harvesting device generated positive voltage and current upon the bending motions (Figure 3b-i and 3b-ii). Figure 3c-i and 3c-ii show the measured negative output peaks for the reverse connection (the inset of Figure 3c-i). In the linear superposition test (see Supporting Information, Figure S5), the output voltage and current signals were improved by serial and parallel connection of two different PMN-PT energy harvesters. On the basis of these results, the measured output was found to be the true pulse produced from the flexible piezoelectric NG devices. A bending stability test was also conducted to confirm the mechanical robustness and durability of the harvester. Figure 3d shows that the output current was measured consistently without noticeable degradation during 30 000 continual bending cycles of the device at a curvature radius of 16.5 mm. This appears to be attributable to

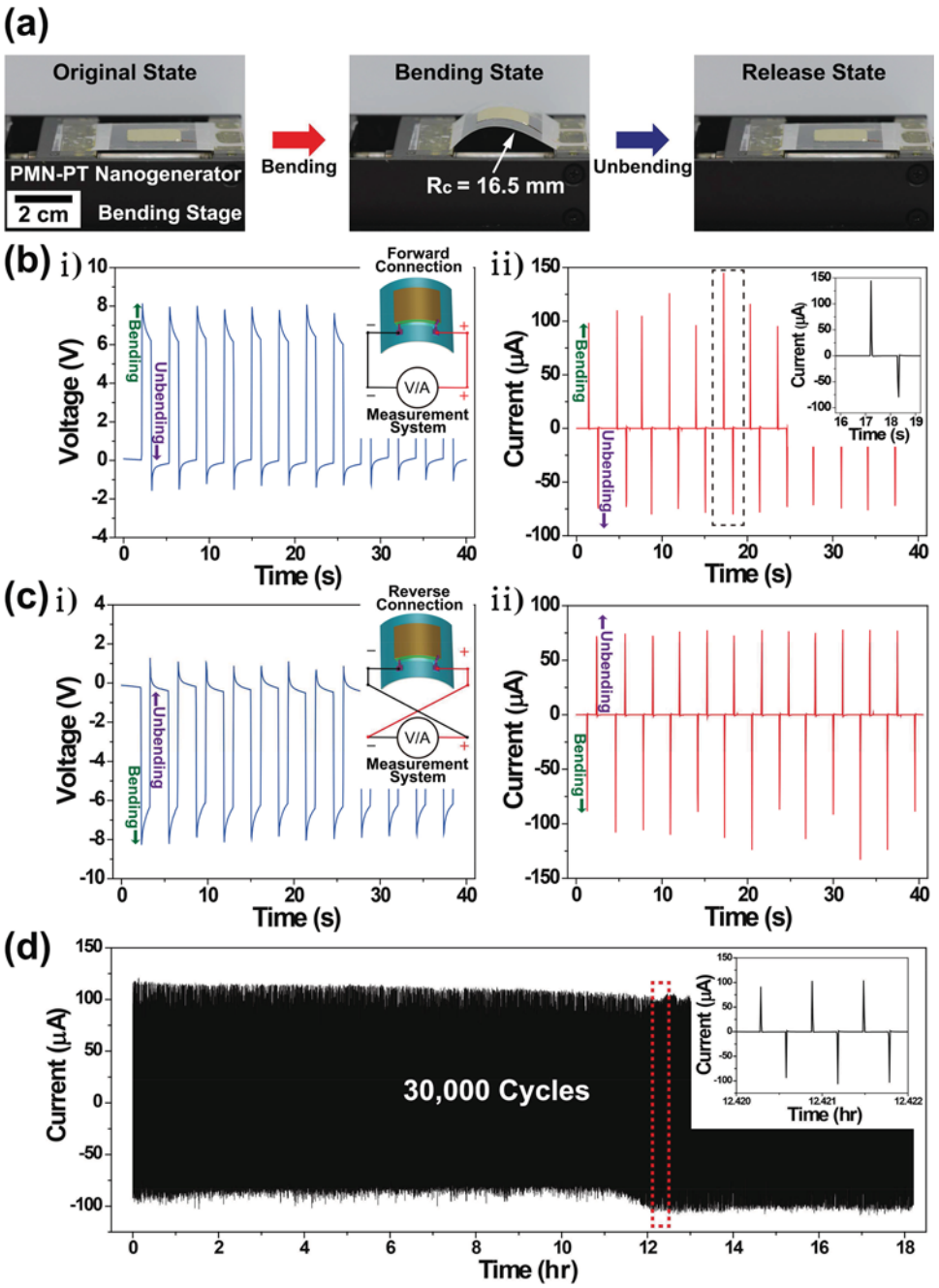

Figure 3. (a) Optical images of the flexible PMN-PT harvesting device in their original, bending, and release states for power generation. (b) The open-circuit voltage (i) and short-circuit current (ii) signals generated from the energy harvester in the forward connection (the inset of Figure 3b-i) during the periodical bending and unbending motions. The inset of Figure 3b-ii shows magnified current peaks. (c) The measured output voltage (i) and current peaks (ii) in the reverse connection (the inset of Figure 3c-i). (d) The result of continuous bending fatigue test up to 30 000 iterations to confirm the mechanical durability of flexible NG device and a zoomed view of red dotted region (the inset).

the sufficient flexibility of thin NG on a plastic substrate under significant fatigue conditions.[41]

To utilize the flexible PMN-PT energy harvester as an additional energy source of an artificial pacemaker, it is necessary to obtain high electric power from the mechanical movement of the flexible device and store the generated electricity.[42] The flexible NG generates alternating current (AC) peaks, which do not match with the DC systems of normal electronic equipment and battery. AC signals were therefore converted into DC signals using a full-wave-bridge-rectification circuit composed of four diodes. The rectified maximum output current and voltage of the device were measured to be approximately 100 μA and 8 V respectively, as shown in **Figure 4**a and 4b. These output values are large enough to directly drive commercial electronics without any subsidiary storage systems. Fifty parallel-connected green LEDs were lighted simultaneously with the generated

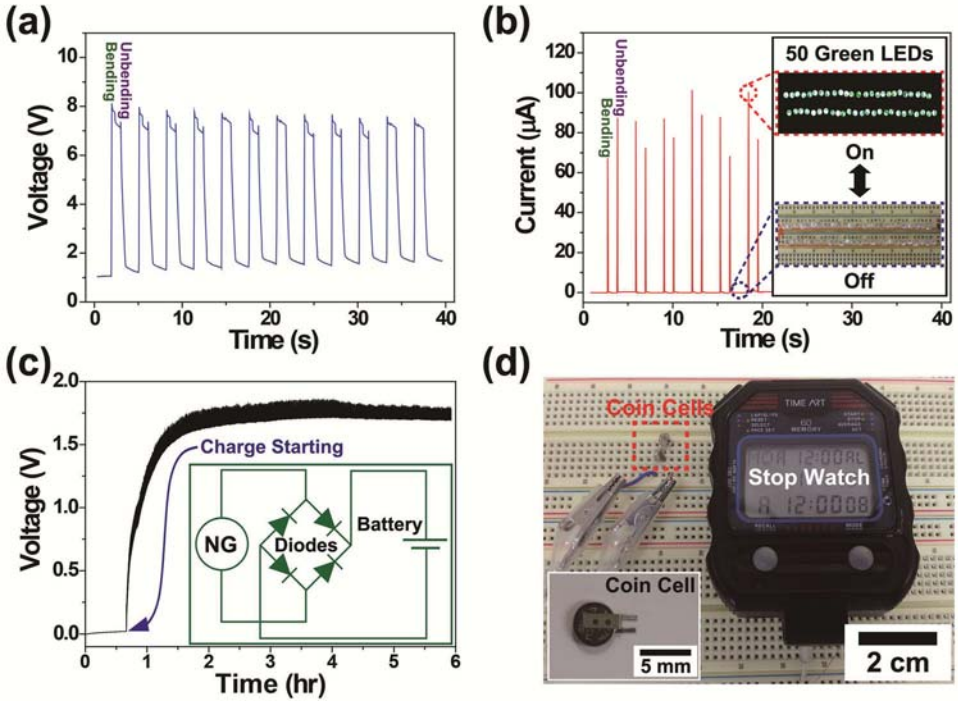

Figure 4. (a) The open-circuit voltage of flexible PMN-PT harvester rectified by bridge diodes. (b) The measured short-circuit current after rectification. The inset shows the lighting up 50 green LEDs, corresponding to the current peaks of NG. (c) The charging curve of a coin battery by the energy harvester. The inset presents a schematic circuit diagram of electric rectifier and energy storage circuit comprising four diodes and a battery. (d) A commercial stop watch operated by the charged two coin cells in series connection. The inset shows an optical image of coin cell charged by the flexible harvesting device.

electric power from the momentary bending and unbending motions of the flexible energy harvester (the inset of Figure 4b, see Video S1 in Supporting Information, the flicker of green LEDs using the flexible PMN-PT NG). The outstanding output current from the piezoelectric harvesting device was advantageous to turn on a series of LED arrays in parallel. Figure 4c shows that a coin cell was charged by the continual bending of flexible PMN-PT harvester (induced strain of 0.36%, strain rate of 2.3%·s^{-1}, and frequency of 0.7 Hz) from 0.05 V to 1.7 V in 3 hours and the inset depicts the equivalent circuit diagram of the connection for energy storage. Figure 4d shows the operation of an electronic device (portable stop watch) by the batteries (the inset of Figure 4d) charged from flexible piezoelectric NG. To switch on the stop watch, two coin cells were connected in series on a bread board since the portable device required a driving voltage of 3 V. This type of energy harvesting and storage system could be used as a potential candidate for the new energy source in artificial pacemakers, thereby resolving intrinsic issues such as increment of battery size or even replacement of discharged batteries.[42,43] The flexible energy harvester studied in the present work could lead to a robust and evolutionary method to longer operation time and miniaturization of batteries, especially in the restricted space of the human body, because they could be readily recharged by cyclic deformation behaviors of biomechanical energy source such as the heartbeat, diaphragm elevation, and elbow bending.[44]

The real-time functional electrical stimulation of the heart by a high output flexible piezoelectric energy harvester has great biomedical importance for a self-powered artificial heart pacemaker.[45] Here, we used the instantaneous electric output of the harvesting device to directly stimulate a rat heart without any external power sources or circuits. **Figure 5**a provides an overall schematic illustration of artificial cardiac pacemaking using a flexible PMN-PT thin film stimulator. The flexible cardiac stimulator was directly linked to stimulation electrodes to provide electrical stimuli to the heart of an anesthetized rat. Three sensing terminals were pinned to the rodent, on the left posterior leg and both anterior legs, to monitor its electrocardiogram (ECG). Figure 5b shows the animal experiment with opening the chest of a rat for stimulation of the heart and perception of the heartbeat. The rat had a typical QRS complex (i.e., QRS is clinically acknowledged as a typical combination of waves related to the heartbeat), P wave, and T wave in the ECG amplitude with a heart rate of about 6 beats per second as displayed in Figure 5c and its inset. In normal animals, external electric energy of 1.1 μJ is minimally needed to trigger the action potential for artificially contracting the heart.[46] When the flexible PMN-PT stimulating device was bent and unbent cyclically, the corresponding spike peaks were observed on the natural heartbeat of the rat in the ECG, as visualized in Figure 5d. The generated energy (2.7 μJ) from one bending motion of the flexible stimulator was larger than the threshold energy (1.1 μJ) to electrically stimulate the living heart (see Supporting Information for the calculation of electric energy from flexible PMN-PT energy harvester, Figure S9). This result shows that the thin film NG has potential biomedical use for the normalization of cardiac function.[47]

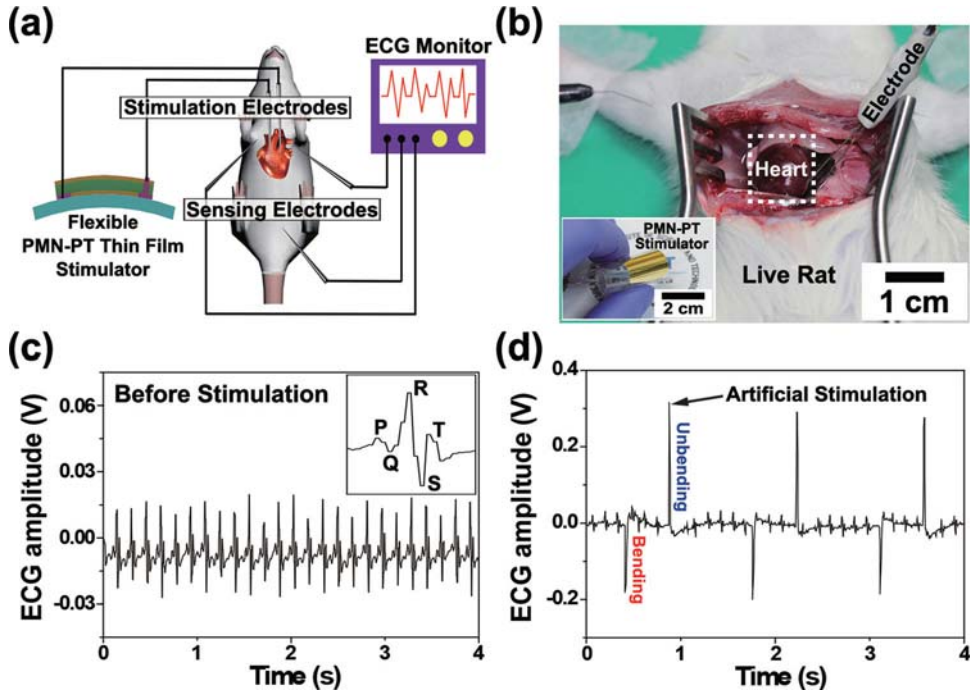

Figure 5. (a) A schematic illustration of the artificial cardiac pacemaking using electrical energy from the flexible PMN-PT energy harvester. (b) A photograph of the medical experiment on a living rat for stimulating the heart. The inset is a snapshot of flexible PMN-PT thin film stimulator being used to stimulate the living heart of rat. (c) The simultaneously recorded ECG in a normal rat heart before the stimulation. The inset presents a magnified heartbeat of the rat, which consists of typical QRS complex, P wave, and T wave. (d) The remarkable artificial peaks on the ECG arise from the stimuli by bending and unbending of the flexible energy harvester.

In summary, a high-performance flexible single crystalline PMN-PT thin film energy harvester was successfully fabricated and applied in a practical demonstration of a self-powered cardiac pacemaker. A mechanical Ni exfoliation process was employed to transfer the entire large area of a single crystal PMN-PT thin film onto a PET substrate from a mother silicon wafer. The PMN-PT NG converted tiny biomechanical motion and mechanical deformation into electric energy with a high current signal of up to 0.223 mA and output voltage of 8.2 V. A FEA simulation theoretically shows that electrical energy can be obtained from stress-induced bending of the flexible piezoelectric harvester. More interestingly, our flexible and thin PMN-PT stimulator was readily implemented in the cardiac muscle of a live rat, enabling real-time functional electrical stimulation. This approach verified that our flexible PMN-PT harvesting device mounted on a thin plastic substrate can be further applicable as a sustainable energy source, which may be able to recharge batteries and stimulate the heart through application to artificial cardiac pacemakers. We are currently planning to investigate three dimensional stacking of piezoelectric thin films on a single plastic substrate and energy harvesting from movement of porcine organs.

Experimental Section

Flexible PMN-PT Thin Film Energy Harvester: (001)-oriented 0.72 PMN - 0.28 PT single crystals were optimized for this work by process of iBULe photonics. Cr/Au (10 nm/100 nm) bottom electrode coated PMN-PT plate was attached to a silicon wafer with an epoxy glue. The PMN-PT thick film was thinned to 8.4 μm of thickness by grinding and CMP, and then Cr/Au (10 nm/100 nm) top electrode was deposited using DC sputtering. After poling process, a 20 μm of Ni stress film was electroplated on PMN-PT thin film in nickel sulfate solution at 50 °C. The Ni/PMN-PT MIM layer was spontaneously exfoliated from the bulk substrate due to inherent tensile stress of the Ni film. The exfoliated layer was bonded on a PET substrate (110 μm) by UV cured adhesive (Norland products), and subsequently the top Ni film was wet-etched in Ni etchant (Transene, TFG). SU-8 (Microchem) layer was optionally coated on the PMN-PT energy harvester to protect the device. The Cu wires were connected on top and bottom electrodes by means of Ag paste for the application of flexible harvesting device and artificial cardiac pacemaker.

Artificial Heart Pacemaking: All animal experiments were performed in compliance with the animal study committee of the Yonsei University, Severance Hospital. A rat was placed under anesthesia with Zoletil 50 (Virbac), and an incision was made on precordium of the rat. The stimulation needles and ECG sensing leads were contacted on left ventricle and rat body, respectively. The flexible thin film stimulator was linked to stimulation electrodes to make artificial heartbeat of live rat using generated electric output from the device.

Supporting Information

Supporting Information is available from the Wiley Online Library or from the author.

Acknowledgements

This work was supported by the Basic Science Research Program (grant code: NRF-2012R1A2A1A03010415, NRF-2010-0021993, NRF-2012R1A2A2A02045367) and Center for Integrated Smart Sensors as

Global Frontier Project (CISS-2012M3A6A6054187) funded by the Korea government (MSIP) through the National Research Foundation of Korea (NRF). This work was also supported by the Small and Medium Business Administration (SMBA) in Korea under contract S2042880.

Received: February 5, 2014
Revised: March 26, 2014
Published online: April 17, 2014

[1] H. G. Mond, J. G. Sloman, R. H. Edwards, *Pacing Clin. Electrophysiol.* **1982**, *5*, 278.
[2] G. D. Nelson, *Texas Heart Institute Journal* **1993**, *20*, 12.
[3] V. S. Mallela, V. Ilankumaran, N. S. Rao, *Indian Pacing and Electrophysiology J.* **2004**, *4*, 201.
[4] F. W. Horlbeck, F. Mellert, J. Kreuz, G. Nickenig, J. O. Schwab, *J. Cardiovasc. Electrophysiol.* **2012**, *23*, 1336.
[5] M. J. Wilhelm, C. Schmid, D. Hammel, S. Kerber, H. M. Loick, M. Herrmann, H. H. Scheld, *Ann. Thorac. Surg.* **1997**, *64*, 1707.
[6] Z. L. Wang, *Adv. Mater.* **2012**, *24*, 280.
[7] K. I. Park, M. Lee, Y. Liu, S. Moon, G. T. Hwang, G. Zhu, J. E. Kim, S. O. Kim, D. K. Kim, Z. L. Wang, K. J. Lee, *Adv. Mater.* **2012**, *24*, 2999.
[8] S. Xu, Y. Qin, C. Xu, Y. G. Wei, R. S. Yang, Z. L. Wang, *Nat. Nanotechnol.* **2010**, *5*, 366.
[9] X. D. Wang, *Am. Ceram. Soc. Bull* **2013**, *92*, 18.
[10] C. Dagdeviren, S. W. Hwang, Y. W. Su, S. Kim, H. Y. Cheng, O. Gur, R. Haney, F. G. Omenetto, Y. G. Huang, J. A. Rogers, *Small* **2013**, *9*, 3398.
[11] K. I. Park, C. K. Jeong, J. Ryu, G. T. Hwang, K. J. Lee, *Adv. Energy Mater.* **2013**, *3*, 1539.
[12] C. K. Jeong, I. Kim, K. I. Park, M. H. Oh, H. Paik, G. T. Hwang, K. No, Y. S. Nam, K. J. Lee, *Acs Nano* **2013**, *7*, 11016.
[13] Z. L. Wang, J. H. Song, *Science* **2006**, *312*, 242.
[14] Y. F. Hu, Y. Zhang, C. Xu, L. Lin, R. L. Snyder, Z. L. Wang, *Nano Lett.* **2011**, *11*, 2572.
[15] C. K. Jeong, K.-I. Park, J. Ryu, G.-T. Hwang, K. J. Lee, *Adv. Funct. Mater.* **2014**, DOI: 10.1002/adfm.201303484.
[16] M. Y. Choi, D. Choi, M. J. Jin, I. Kim, S. H. Kim, J. Y. Choi, S. Y. Lee, J. M. Kim, S. W. Kim, *Adv. Mater.* **2009**, *21*, 2185.
[17] Y. F. Hu, L. Lin, Y. Zhang, Z. L. Wang, *Adv. Mater.* **2012**, *24*, 110.
[18] K. I. Park, S. Xu, Y. Liu, G. T. Hwang, S. J. L. Kang, Z. L. Wang, K. J. Lee, *Nano Lett.* **2010**, *10*, 4939.
[19] J. Kwon, W. Seung, B. K. Sharma, S. W. Kim, J. H. Ahn, *Energ. Environ. Sci.* **2012**, *5*, 8970.
[20] K.-I. Park, J. H. Son, G.-T. Hwang, C. K. Jeong, J. Ryu, M. Koo, I. Choi, S. H. Lee, M. Byun, Z. L. Wang, K. J. Lee, *Adv. Mater.* **2014**, *26*, 2154.
[21] M. Southcott, K. MacVittie, J. Halamek, L. Halamkova, W. D. Jemison, R. Lobel, E. Katz, *Phys. Chem. Chem. Phys.* **2013**, *15*, 6278.
[22] S. Y. Xu, Y. W. Yeh, G. Poirier, M. C. McAlpine, R. A. Register, N. Yao, *Nano Lett.* **2013**, *13*, 2393.
[23] M. Lucas, W. J. Mai, R. S. Yang, Z. L. Wang, E. Riedo, *Nano Lett.* **2007**, *7*, 1314.
[24] S. W. Bedell, K. Fogel, P. Lauro, D. Shahrjerdi, J. A. Ott, D. Sadana, *J. Phys. D Appl. Phys.* **2013**, 46.
[25] S. G. Lee, R. G. Monteiro, R. S. Feigelson, H. S. Lee, M. Lee, S. E. Park, *Appl. Phys. Lett.* **1999**, *74*, 1030.
[26] H. S. Luo, G. S. Xu, H. Q. Xu, P. C. Wang, Z. W. Yin, *Japanese Journal of Applied Physics* **2000**, *39*, 5581.
[27] S. Kamba, E. Buixaderas, J. Petzelt, J. Fousek, J. Nosek, P. Bridenbaugh, *J. Appl. Phys.* **2003**, *93*, 933.
[28] Y. J. Zhai, L. Mathew, R. Rao, D. W. Xu, S. K. Banerjee, *Nano Lett.* **2012**, *12*, 5609.
[29] D. H. Kim, J. Viventi, J. J. Amsden, J. L. Xiao, L. Vigeland, Y. S. Kim, J. A. Blanco, B. Panilaitis, E. S. Frechette, D. Contreras, D. L. Kaplan, F. G. Omenetto, Y. G. Huang, K. C. Hwang, M. R. Zakin, B. Litt, J. A. Rogers, *Nat. Mater.* **2010**, *9*, 511.
[30] L. P. Chen, J. Gao, *Epl-Europhys. Lett.* **2011**, 93.
[31] G. T. Hwang, D. Im, S. E. Lee, J. Lee, M. Koo, S. Y. Park, S. Kim, K. Yang, S. J. Kim, K. Lee, K. J. Lee, *Acs Nano* **2013**, *7*, 4545.
[32] Z. Y. Feng, D. Q. Shi, S. X. Dou, *Solid State Commun.* **2011**, *151*, 123.
[33] J. Kim, Y. Kim, Y. S. Kim, J. Lee, L. Kim, D. Jung, *Appl. Phys. Lett.* **2002**, *80*, 3581.
[34] I. R. Henderson, *Piezoelectric Ceramics: Principles and Applications* APC International Ltd., PA, USA **2006**.
[35] A. Nechibvute, A. Chawanda, P. Luhanga, *ISRN Materials Science* **2012**, 2012.
[36] R. S. Yang, Y. Qin, L. M. Dai, Z. L. Wang, *Nat. Nanotechnol.* **2009**, *4*, 34.
[37] S. I. Park, J. H. Ahn, X. Feng, S. D. Wang, Y. G. Huang, J. A. Rogers, *Adv. Funct. Mater.* **2008**, *18*, 2673.
[38] J. D. Baniecki, R. B. Laibowitz, T. M. Shaw, K. L. Saenger, P. R. Duncombe, C. Cabral, D. E. Kotecki, H. Shen, J. Lian, Q. Y. Ma, *J. Eur. Ceram. Soc.* **1999**, *19*, 1457.
[39] J. Tian, P. Han, D. A. Payne, *IEEE T. on* **2007**, *54*, 1895.
[40] G. H. Haertling, *J. Am. Ceram. Soc.* **1999**, *82*, 797.
[41] S. Kim, H. Y. Jeong, S. K. Kim, S. Y. Choi, K. J. Lee, *Nano Lett.* **2011**, *11*, 5438.
[42] S. H. Wang, L. Lin, Z. L. Wang, *Nano Lett.* **2012**, *12*, 6339.
[43] G. Anastasia, M. Contib, M. D. Francescoa, A. Passarella, *Ad Hoc Netw.* **2009**, *7*, 537.
[44] C. Pan, Z. Li, W. Guo, J. Zhu, Z. L. Wang, *Angew. Chem.* **2011**, *123*, 11388.
[45] G. Zhu, A. C. Wang, Y. Liu, Y. S. Zhou, Z. L. Wang, *Nano Lett.* **2012**, *12*, 3086.
[46] T. E. Starzl, R. A. Gaertner, R. C. Webb Jr., *Circulation* **1955**, *11*, 952.
[47] L. Gu, N. Y. Cui, L. Cheng, Q. Xu, S. Bai, M. M. Yuan, W. W. Wu, J. M. Liu, Y. Zhao, F. Ma, Y. Qin, Z. L. Wang, *Nano Lett.* **2013**, *13*, 91.